DETC2007-34411

FREQUENCY LOCKING IN A FORCED MATHIEU-VAN DER POL-DUFFING SYSTEM

Manoj Pandey
Dept. TAM
Cornell University
Ithaca NY 14853
Email: mp252@cornell.edu

Richard H. Rand
Dept. TAM
Cornell University
Ithaca NY 14853
Email: rhr2@cornell.edu

Alan T. Zehnder
Dept. TAM
Cornell University
Ithaca NY 14853
Email: atz2@cornell.edu

ABSTRACT

Optically actuated Radio Frequency MEMS devices are seen to self oscillate or vibrate under illumination of sufficient strength [1]. These oscillations can be frequency locked to a periodic forcing, applied through an inertial drive at the forcing frequency, or subharmonically via a parametric drive, hence providing tunability. In a previous work [2] this MEMS device was modeled by a three dimensional system of coupled thermomechanical equations requiring experimental observations and careful finite element simulations to obtain the model parameters. The resulting system of equations is relatively computationally expensive to solve which could impede its usage in a complex network of such resonators. In this paper we present a simpler model which shows similar behavior to the MEMS device. We investigate the dynamics of a Mathieu-van der Pol-Duffing equation, which is forced both parametrically and nonparametrically. It is shown that the steady state response can consist of either 1:1 frequency locking, or 2:1 subharmonic locking, or quasiperiodic motion. The system displays hysteresis when the forcing frequency is slowly varied. We use perturbations to obtain a slow flow, which is then studied using the bifurcation software package AUTO.

INTRODUCTION

Tunable limit cycle MEMS oscillators and resonators are becoming important components in RF microsystems where they are used as electromechanical filters [3], amplifiers and nonlinear mixers [4]. They also find use in different kinds of scanning probe microscopes [5,6], as well as biological and chemical sensors [7].

In previous works MEMS devices consisting of a thin, planar, radio frequency resonator [1, 2, 8, 9] were studied. These devices were shown to self-oscillate in the absence of external forcing, when illuminated by a DC laser of sufficient amplitude. This system can also be forced externally either parametrically, by modulating the incident laser, or nonparametrically, by using a piezo drive at the natural frequency of the device. In the presence of external forcing of sufficient strength and close enough in frequency to that of the unforced oscillation, the device will become frequency locked or get entrained by the forcer. A model was presented in [1, 2, 8, 9] which consisted of a third order system of ODE's. Figure 1 shows the experimentally observed amplitude and frequency response close to entrainment. The limit cycle oscillation is entrained by the forcing, close to the natural frequency of the oscillator. Parametric variation of the entrainment region as a function of forcing amplitude is shown in Figure 1c. The outer boundaries in Figure 1c separate entrained regions from quasi-periodic response.

In this paper a simpler model is studied, which still shows all the relevant phenomena seen in the disc resonator, namely limit cycles, parametric excitation and nonparametric excitation. The essential features of the entrainment in a disc resonator can be listed as follows:

1. For a DC laser of sufficient power, the disc resonator starts to self oscillate at constant amplitude. The simplest canonical model which captures this behavior is a van der Pol (vdP) oscillator [10]. It consists of an $-\varepsilon\dot{x}(1-x^2)$ term added to a 1D simple harmonic oscillator (SHO), which in the absence of forcing leads to a steady state vibration called a limit cycle. For small values of ε the limit cycle has frequency close to 1, which is the

frequency of the unforced linear oscillator.

2. The limit cycle in the system can be periodically forced either parametrically, by modulating the laser, or nonparametrically, by using a piezo drive. The Mathieu equation [10], which consists of adding a $\varepsilon\alpha\cos(2\omega t)x$ term to a 1D SHO, can model parametric forcing of the system applied at twice the natural frequency of the resonator. This term in the absence of the vdP term, renders the origin unstable when the parametric forcing frequency 2ω is close to twice the frequency of the unforced linear oscillator. Nonparametric forcing can be modeled by a term of form $F_0\sin\omega t$.

3. When entrained, the system shows a backbone-shaped amplitude vs forcing frequency response. This kind of behavior is typical of the large amplitude response of structures and can be modeled by a Duffing's equation term [10], $\varepsilon\beta x^3$, added to the SHO.

This paper concerns the following differential equation, which may be thought of as a forced Mathieu-van der Pol-Duffing equation:

$$\ddot{x}+(1+\varepsilon\alpha\,\cos(2\omega t+\phi))x-\varepsilon\dot{x}(1-x^2)+\varepsilon\beta x^3=\varepsilon F\,\cos\omega t \quad (1)$$

where $\varepsilon\alpha$ is the magnitude of parametric forcing applied at frequency 2ω, and εF is the magnitude of nonparametric forcing applied at frequency ω while ϕ is the phase difference between the parametric and the nonparametric forcing. β is the coefficient of the cubic nonlinearity term and ε is a small parameter which will be used in the perturbation method. Eq.(1) is combination of a van der Pol (vdP) equation term [10], $-\varepsilon\dot{x}(1-x^2)$, a Mathieu equation term [10], $\varepsilon\alpha\cos(2\omega t)x$, and Duffing's equation term, $(\varepsilon\beta x^3)$, added to a forced SHO.

NUMERICAL SIMULATIONS

Numerical results and subsequent analysis are presented for two cases. To begin with, only non-parametric excitation is applied to the system. This corresponds to using $\alpha=0$ in equation 1. The numerical results in Figure 2 show that as ω is increased (quasistatically) from 1, the response first consists of a quasiperiodic motion, which is a combination of contributions from the limit cycle and from the forcing. As the frequency is swept forward, the relatively-constant amplitude quasiperiodic motion suddenly jumps onto a single frequency response which increases in amplitude with a further increase in the forcing frequency. Beyond a certain forcing frequency (around $\omega=1.13$ in Figure 2) the motion jumps back to the lower amplitude quasiperiodic response. Hysteresis is seen when the frequency is swept back. This response is similar to the experimentally obtained response for the disk resonator.

Next the parametric forcing is also switched on and response amplitude as a function of forcing frequency ω for a case with parameters $\varepsilon=0.1$, $\alpha=1$, $F=0.3$, $\beta=0.0$ and $\phi=0$ is shown

in Figure 3. The cubic nonlinearity (β) is not considered here to simplify the subsequent analysis. Quasiperiodic behavior (QP) is observed in the regions located approximately at $\omega<0.97$ and $\omega>1.03$. Periodic behavior at the forcing frequency is observed in the rest of the plot, corresponding to entrainment. As we sweep the frequency forward inside the entrained region, the amplitude jumps to a higher value at a frequency $\omega\approx1.015$. No comparable jump is seen when the frequency is swept backward, indicating hysteresis.

We note that the parameters used in Figures 2 and 3 have been chosen to illustrate the hysteresis exhibited by the model system of Equation 1, and are not obtained from the MEMS device referred to in Figure 1.

PERTURBATION SCHEME

We use the two variable expansion method (also known as the method of multiple scales) to obtain an approximate analytic solution for equation 1. The idea of this method is to replace time t by two time scales, $\xi=\omega t$, called stretched time, and $\eta=\varepsilon t$, called slow time. The forcing frequency ω is expanded around the natural frequency of the oscillator ($\omega=1$), i.e.

$$\omega=1+k_1\varepsilon+O(\varepsilon^2) \quad (2)$$

where k_1 is a detuning parameter at order ε. Next, x is expanded in a power series in ε:

$$x=x_0(\xi,\eta)+\varepsilon x_1(\xi,\eta)+O(\varepsilon^2) \quad (3)$$

Substituting Equations 2,3 into 1 and collecting terms gives:

$$x_{0\xi\xi}+x_0=0 \quad (4)$$

$$x_{1\xi\xi}+x_1=\,-2k_1 x_{0\xi\xi}-2x_{0\xi\eta}+(1-x_0^2)x_{0\xi}$$
$$-\alpha x_0\cos(2\xi+\phi)-\beta x_0^3+F\cos\xi \quad (5)$$

We take the solution to Equation 4 in the form:

$$x_0(\xi,\eta)=A(\eta)\,\cos\xi+B(\eta)\,\sin\xi \quad (6)$$

Substitution of Equation 6 into 5 and removal of secular terms gives the following slow flow, where primes represent differentiation with respect to η:

$$A' = -Bk_1 + \frac{A}{2} - \frac{A}{8}(A^2+B^2) - \frac{\alpha}{4}(A\sin\phi + B\cos\phi)$$
$$+ \frac{3\beta B}{8}(B^2+A^2) \tag{7}$$

$$B' = Ak_1 + \frac{B}{2} - \frac{B}{8}(A^2+B^2) - \frac{\alpha}{4}(A\cos\phi - B\sin\phi)$$
$$- \frac{3\beta A}{8}(B^2+A^2) + \frac{F}{2} \tag{8}$$

From Equation 6 we see that a fixed point in the slow flow corresponds to a periodic motion in the original equation, while a limit cycle in the slow flow corresponds to a quasiperiodic motion in the original equation.

PERTURBATION RESULTS FOR NONPARAMETRIC EXCITATION

In this section results are shown for the case when parametric forcing is switched off (α=0). The slow flow in this case reduces to

$$A' = -Bk_1 + \frac{A}{2} - \frac{A}{8}(A^2+B^2) + \frac{3\beta B}{8}(B^2+A^2) \tag{9}$$

$$B' = Ak_1 + \frac{B}{2} - \frac{B}{8}(A^2+B^2) - \frac{3\beta A}{8}(B^2+A^2) + \frac{F}{2} \tag{10}$$

See Figure 4 which shows the results of applying the continuation software AUTO [11] to Equations 9 and 10. The amplitude of the fixed point and the radius of the limit cycle are displayed as functions of forcing frequency. The phase plane plots associated with different regions are also shown.

As expected, away from the resonance a limit cycle is seen to coexist with an unstable fixed point, which is close to zero. As the forcing frequency gets closer to the resonant frequency, the unstable fixed point increases in amplitude and undergoes supercritical Hopf bifurcation at point 1, becoming a stable fixed point in the process. The stable limit cycle disappears at this point and the motion jumps onto the stable fixed point. If the forcing frequency continues to increase (quasistatically), the system follows the resonance curve in Figure 4 from point 1 to point 3, increasing in amplitude all the while. For these values of ω, the system is said to be entrained by the forcing function since it responds at the forcing frequency. A saddle point arises at point 4 from a

saddle node bifurcation and has amplitude close to but lower than the mentioned stable fixed point of the resonance curve. The stable fixed point disappears next in a saddle node bifurcation with the saddle point, close to the resonance curve at point 3. Further increases in ω beyond point 3 cause the motion to jump back to the limit cycle, producing quasiperiodic motion which involves both the frequency of the forcer and the frequency of the unforced limit cycle. When the frequency is swept back, it is clear that the point at which the limit cycle would be entrained must be different from the point at which the resonance curve disappears. The entrainment in this case is achieved when the limit cycle undergoes a fold by coalescing with an unstable limit cycle which is born in a homoclinic bifurcation near point 4 and hence the motion jumps back to the stable fixed point at 4. The system then follows the resonance curve until the Hopf bifurcation point 1. Hysteresis is seen in the dependence of the entrainment region on the direction of sweep.

PERTURBATION RESULTS FOR PARAMETRIC EXCITATION

In this section we study the effect of switching on the parametric forcing ($\alpha \neq 0$). We set $\beta = 0$ (no Duffing x^3 term) to simplify the analysis. Thus 7 and 8 reduce to following

$$A' = -Bk_1 + \frac{A}{2} - \frac{A}{8}(A^2+B^2) - \frac{\alpha}{4}(A\sin\phi + B\cos\phi) \tag{11}$$

$$B' = Ak_1 + \frac{B}{2} - \frac{B}{8}(A^2+B^2) - \frac{\alpha}{4}(A\cos\phi - B\sin\phi) + \frac{F}{2} \tag{12}$$

Invariances of the slow flow

The slow flow 11,12 contains 4 parameters: detuning k_1, parametric forcing amplitude α, nonparametric forcing amplitude F and the phase difference ϕ. We shall be interested in understanding how the phase portrait of the slow flow is determined by these parameters. However, before discussing this we note that Equations 11,12 exhibit some invariances which permit useful conclusions to be drawn. For example, 11,12 remain unchanged when A, B and F are replaced respectively by $-A$, $-B$ and $-F$. Since such a change does not alter the nature of the phase portrait, we see that *we may consider $F \geq 0$ without loss of generality*.

In addition, we see that Equations 11 and 12 remain unchanged when A, k_1, α and ϕ are replaced respectively by $-A$, $-k_1$, $-\alpha$ and $-\phi$. Since changing the sign of A does not alter the nature of the phase portrait, we see that *we may consider $\alpha \geq 0$ without loss of generality* since negative α just reverses the k_1 and ϕ axes in the $k_1 - F - \phi$ bifurcation diagram, which leaves it essentially unchanged.

By the same reasoning, we may consider $\phi \geq 0$ without loss of generality, since replacing ϕ by -ϕ leaves the $k_1 - F - \alpha$ bifurcation diagram essentially unchanged. However since Equations

3

11,12 are 2π-periodic in ϕ, we may equally well choose ϕ to lie in any interval of length π. *Hence we may consider* $-\frac{\pi}{2} < \phi < \frac{\pi}{2}$ *without loss of generality.*

Parametric Study

Figure 5 shows the results of the AUTO [11] analysis for $\alpha = 1$ and $\phi = 0$, where k_1 and F are varied. Region A contains 5 slow flow equilibria, consisting of 2 sinks, 2 saddles and 1 source, i.e., only 2 are stable. These stable equilibria correspond to frequency locked periodic motions in Equation 1. The presence of two such steady states signals the possibility of hysteresis. This same (stable) steady state occurs in region D, which lies above region A in Figure 5. The difference between these two regions is that D contains only 3 slow flow equilibria, namely 2 sinks and a saddle. As we cross the curve separating A and D, two of the saddles in A merge with the source in A in a pitchfork bifurcation, leaving a single saddle in their place.

We next consider regions E and B which lie to the left and right of region A in Figure 5. The slow flow phase portrait for points in these two regions are qualitatively the same, consisting of 3 slow flow equilibria, namely a source, a saddle and a sink. Only one of these slow flow equilibria is stable, and corresponds to a periodic motion at the forcing frequency in Equation 1. This same (stable) steady state occurs in region C_2, which lies above region D in Figure5. The difference between region C_2 and regions E and B is that C_2 contains just 1 slow flow equilibrium point, namely a sink. As we cross the curve separating C_2 from one of the regions E, D or B below it (each of which contains 3 slow flow equilibria), a saddle-node bifurcation occurs leaving a single sink in region C_2.

We have now discussed all regions in Figure 5 except for regions C_1 which lie in the lower left and right portions of Figure 5. Regions C_1 contain a single unstable slow flow equilibrium point, namely a source. However, unlike the other regions in Figure 5, regions C_1 also contain a stable slow flow limit cycle. This motion corresponds to a stable quasiperiodic motion in Equation 1. Hopf bifurcations occur along the curves separating regions C_1 and C_2.

We offer the following summary of predicted (stable) steady state behavior of Equation 1: In regions A and D we have 2 distinct stable periodic motions; in regions E, C_2 and B we have a single stable periodic motion; and in regions C_1 we have a stable quasiperiodic motion.

The discussion thus far has fixed α at unity (Figure 5). We next look at the effect of changing α. See Figure 6. We see that the width of the region corresponding to 2 distinct steady state periodic motions (regions A and D) decreases as we decrease α. In addition the regions B and E become more symmetrical. For $\alpha = 0.2$ we see that the region D has disappeared and the regions E and B have merged to give just one region. At $\alpha = 0$ the region with 2 stable steady states has disappeared. This case

corresponds to nonparametric periodic forcing of a van der Pol oscillator, and has been discussed in [12].

Thus the presence of the regions A and D which contain 2 stable periodic motions may be associated with the parameter α. Since α is the coefficient of the parametric excitation term which has frequency 2ω, we may associate these regions with 2:1 subharmonic response. This is in contrast to regions E, B and C_2, which may be associated with 1:1 frequency locking.

The dependence of the bifurcation curves of Figure 5 on ϕ is displayed in Figure 7. The diagram is seen to be symmetric about $k_1 = 0$ for $\phi = \frac{\pi}{2}$ and $\phi = -\frac{\pi}{2}$. As long as the nonparametric forcing leads the parametric forcing (i.e. $-\frac{\pi}{2} < \phi < 0$), decreasing phase magnitude $|\phi|$ bends the region of 2:1 entrainment (regions A and D) to the left. As a result, region E becomes very small for $\phi = 0$. On the other hand when the parametric forcing leads the nonparametric forcing (i.e. $0 < \phi < \frac{\pi}{2}$), increasing ϕ causes region E to increase in size at the expense of region D, until at $\phi = \frac{\pi}{2}$ region D completely disappears and the region E is the same size as B. For values of ϕ in the range $[\frac{\pi}{2}, \frac{3\pi}{2}]$, the $k_1 - F$ bifurcation diagram is essentially the same as shown in Figure 7, as discussed earlier in the section on invariances of the slow flow.

CONCLUSION

In this paper we have presented the analysis of entrainment behavior in simplified canonical models of forced limit cycle oscillators. We showed that these models captured many details of the steady state response of a MEMS disk oscillator which had been studied in previous works. The models studied in this paper are substantially simpler than the third order system of ODE's which was previously used to model the MEMS device, and as a result, the models presented here are expected to be more useful in studies of networks of coupled disk oscillators.

In the case of nonparametric excitation, we treated a forced van der Pol-Duffing system, Equation 1 with $\alpha=0$, which exhibited a limit cycle being entrained by a periodic forcing function when the forcing frequency is close to the natural frequency of the system. In particular, Figure 4 shows how the classic amplitude-frequency relation of the forced Duffing equation becomes modified when the unforced system exhibits a limit cycle.

In the case of parametric excitation, we treated a forced Mathieu-van der Pol system, Equation 1 with $\beta = 0$, which exhibited either 2:1 subharmonic motion, or 1:1 periodic motion, or quasiperiodic motion, depending on the forcing frequency and the forcing amplitudes, both parametric and nonparametric. The findings may be summarized briefly in words (for fixed α) by stating that parametric excitation is most important when ω is close to the unforced frequency of the oscillator (here taken as unity), or, in other words, when the detuning k_1 is close to zero, and when F is small. Nonparametric forcing takes over when $|k_1|$ is a little larger or when F is larger. Quasiperiodic behavior

4

occurs when $|k_1|$ becomes sufficiently large for given F.

Finally we note that the hysteresis observed using slowly varying forcing frequency, in both experiments (Figure 1) and in numerical simulations (Figure 2 and Figure 3), is explained by changes in the nature of the steady state due to bifurcations in the slow flow equilibria. For example, the jump upwards in Figure 3 is due to passage from region A to region B in Figure 5, in the process of which a saddle-node bifurcation occurs and a stable periodic motion disappears.

ACKNOWLEDGEMENT

REFERENCES

[1] *Aubin K.L., Pandey M., Zehnder A.T., Rand R.H., Craighead H.G., Zalalutdinov, M. and J.M. Parpia. Frequency entrainment for micromechanical oscillator.* Applied Physics Letters, *83:3281–3283, 2003.*

[2] *Keith Aubin, Maxim Zalalutdinov, Tuncay Alan, Robert Reichenbach, Richard Rand, Alan Zehnder, Jeevak Parpia, and Harold Craighead. Limit cycle oscillations in cw laser driven nems.* IEEE/ASME Journal of Micromechanical Systems, *13:1018–1026, 2004.*

[3] *A.-C. Wong, Nguyen C.T.-C, and H. Ding. Rf mems for wireless applications.* IEEE Intl. Solid-State Circuits Conference, *448:78, 1999.*

[4] *Keith L. Aubin, Maxim Zalautdinov, Robert B. Reichenbach, Brian Houston, Alan T. Zehnder, Jeevak M. Parpia, and Harold G. Craighead. Laser annealing for high-q mems resonators.* Proceedings of SPIE, *5116:531–535, 2003.*

[5] *Scherer V., Hartmann U., Goldade A., Bhushan B., Reinstadtler M., Rabe U. and Arnold W. On the nanoscale measurement of friction using atomic-force microscope cantilever torsional resonances.* Applied Physics Letters, *82:2604–2606, 2003.*

[6] *K. J. Bruland, D. Rugar, O. Zuger, S. Hoen, J. A. Sidles, J. L. Garbini and C. S. Yannoni. Magnetic resonance force microscopy.* Review of Mordern Physics, *67:249, 1995.*

[7] *D. Sarid.* Scanning Force Microscopy With Applications to Electric, Magnetic and Atomic Forces. *Oxford University Press, New York, 1994.*

[8] *M. Pandey, K. Auburn, M. Zalalutdinov, R.B. Reichenbach, A.T. Zehnder, R.H. Rand and H.G. Craighead. Analysis of frequency locking in optically driven mems resonators.* IEEE Journal of Microelectromechanical Systems, *15:1546-1554, 2006.*

[9] *Manoj Pandey, Richard Rand, and Alan Zehnder. Perturbation analysis of entrainment in a micromechanical limit cycle oscillator.* Communications in Nonlinear Sciences and Numerical Simulation, *12:1291-1301, 2007.*

[10] *A.H. Nayfeh and D.T. Mook.* Nonlinear Oscillations. *Wiley-Interscience, NY, 1979.*

[11] *Paffenroth R.C., Champneys A.R., Fairgrieve T.F., Kuznetsov Y.A., Oldeman B.E., Sandstede B., Doedel, E.J. and X. Wang.* AUTO 2000: Continuation and Bifurcation Software for Ordinary Differential Equations. *available on line at: http://sourceforge.net/project/showfiles.php?group_id = 21781, 2002.*

[12] *R.H. Rand. Lecture Notes in Nonlinear Vibrations* (version 45). *Published on-line by The Internet-First University Press, Ithaca, NY, http://dspace.library.cornell.edu/handle/1813/79, 2004.*
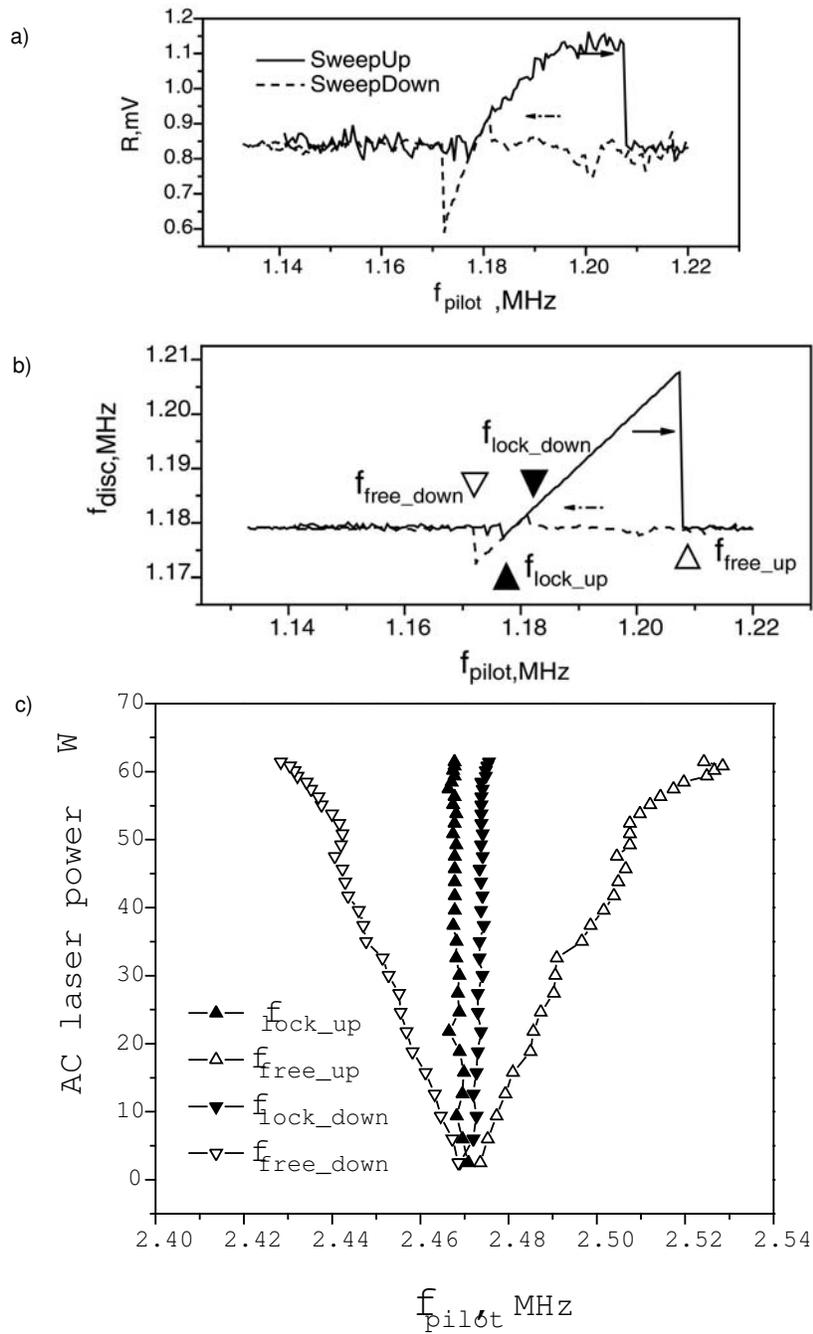
Figure 1. Experimental results for entrainment in a CW laser driven, limit-cycle, disc resonator. a) Amplitude response and b) frequency response obtained when sweeping the frequency of inertial drive. c) Entrainment region obtained when sweeping the modulation frequency of the incident laser about 2ω with no inertial drive. From [2].
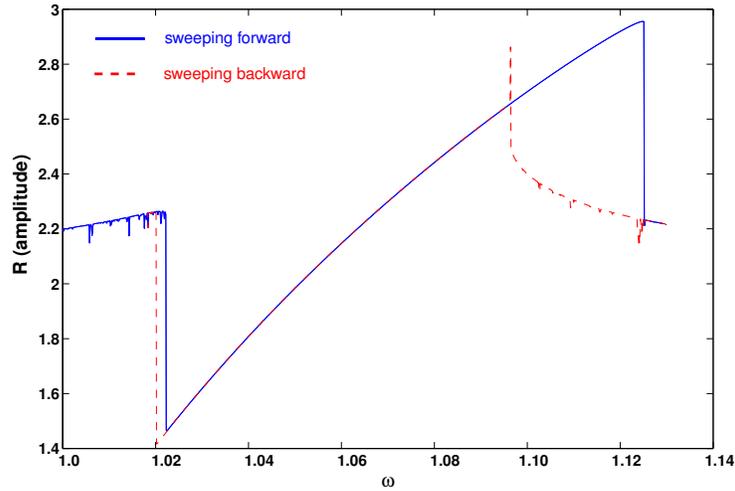
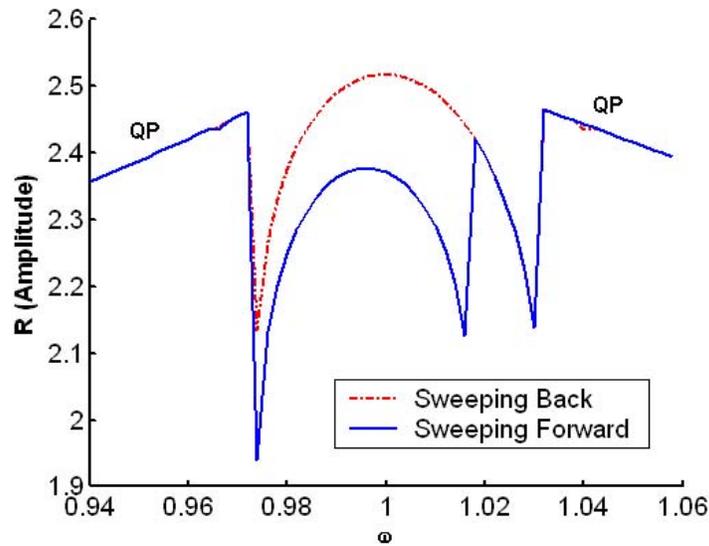Figure 2. Steady state solution obtained be numerical integration of equation 1 . F=3.0, β=3.75,α=0.0 and ε=0.1.

Figure 3. Results of numerical integration of equation 1 for parameters $\varepsilon = 0.1$, $\alpha = 1$,β=0, F = 0.3 and $\phi = 0$. Response amplitude R is plotted against forcing frequency ω. Quasiperiodic behavior (QP) is observed in the regions located approximately at $\omega < 0.97$ and $\omega > 1.03$. Periodic behavior at the forcing frequency is observed in the rest of the plot, with hysteresis as shown.
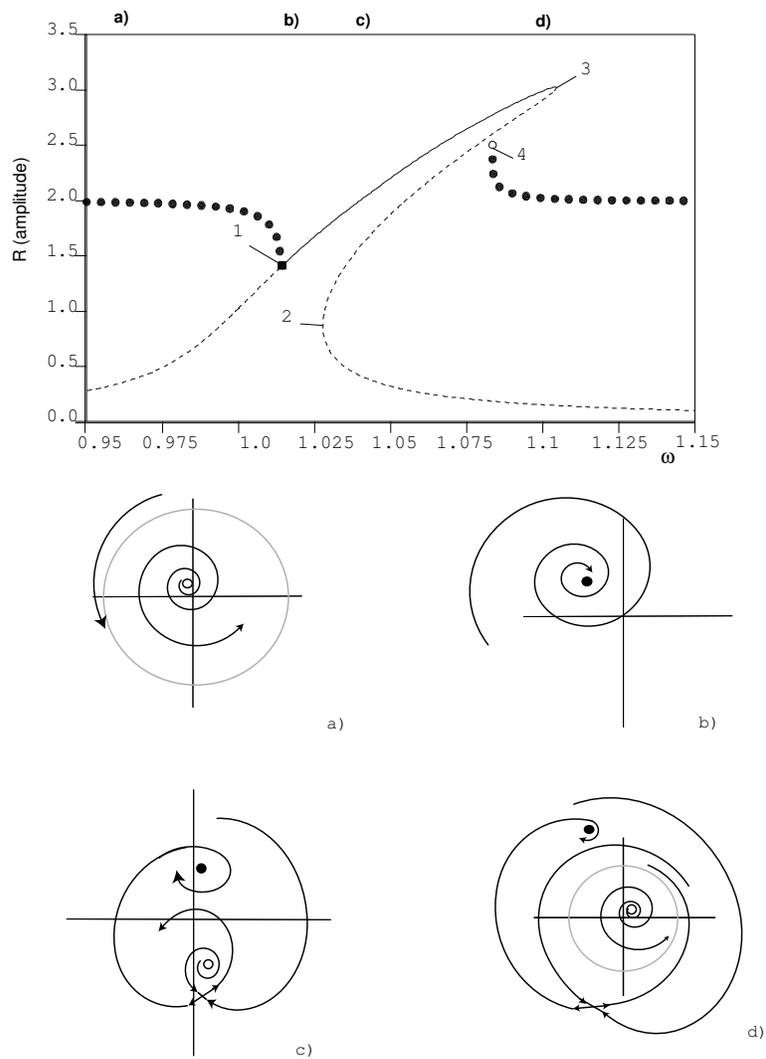
Figure 4. Perturbation results obtained by applying the continuation software AUTO to equations 9, 10. F=3.0, β=3.75 and ε=0.1. The darkly dotted curves signify limit cycles in the slow flow, which correspond to quasiperiodic motions in the original equation.
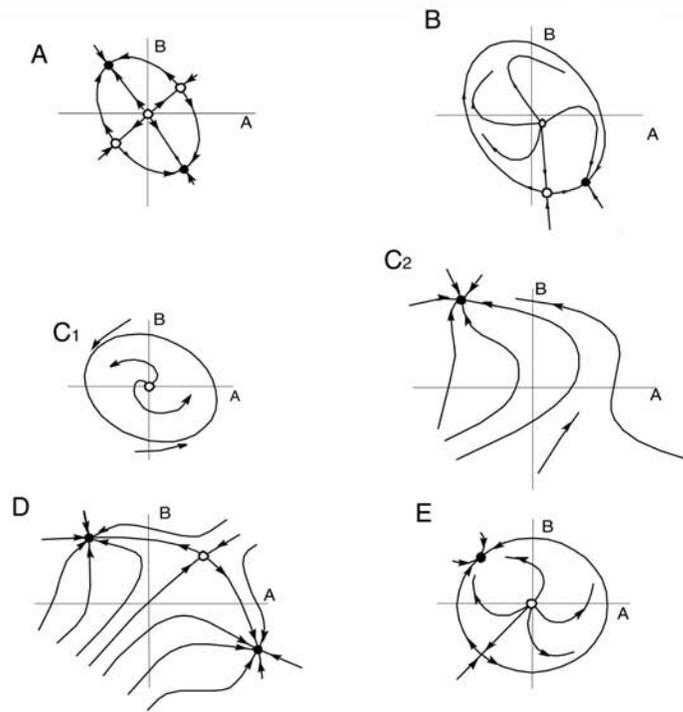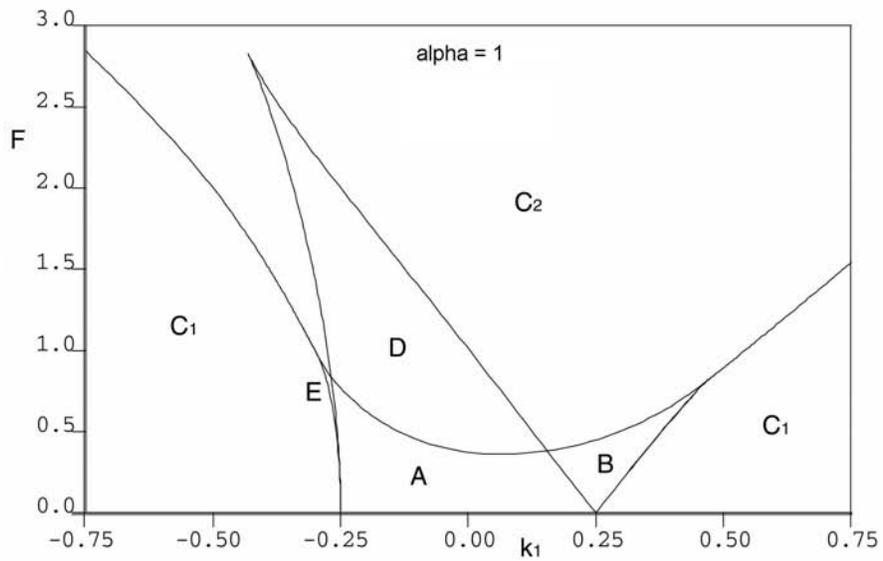
Figure 5. Behavior of the slow flow 11,12. Bifurcation curves (obtained using AUTO) and sketches of corresponding slow flow phase portraits are displayed for $\alpha = 1$ and $\phi = 0$.
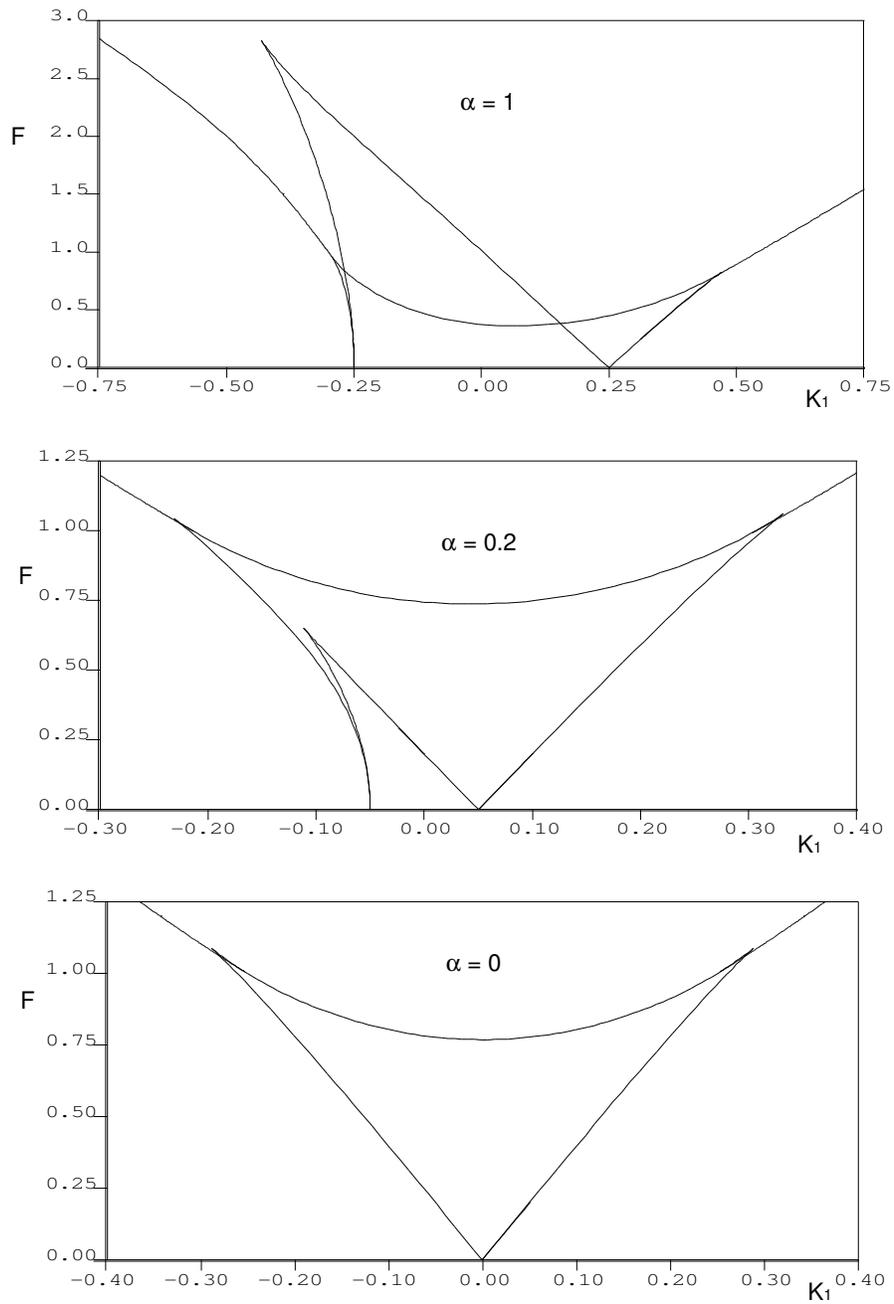
Figure 6. Bifurcation curves (obtained using AUTO) for slow flow 11,12 for α = 1, 0.2 and 0. ϕ = 0 in all the cases. The top subfigure is the same as that in Figure 5.
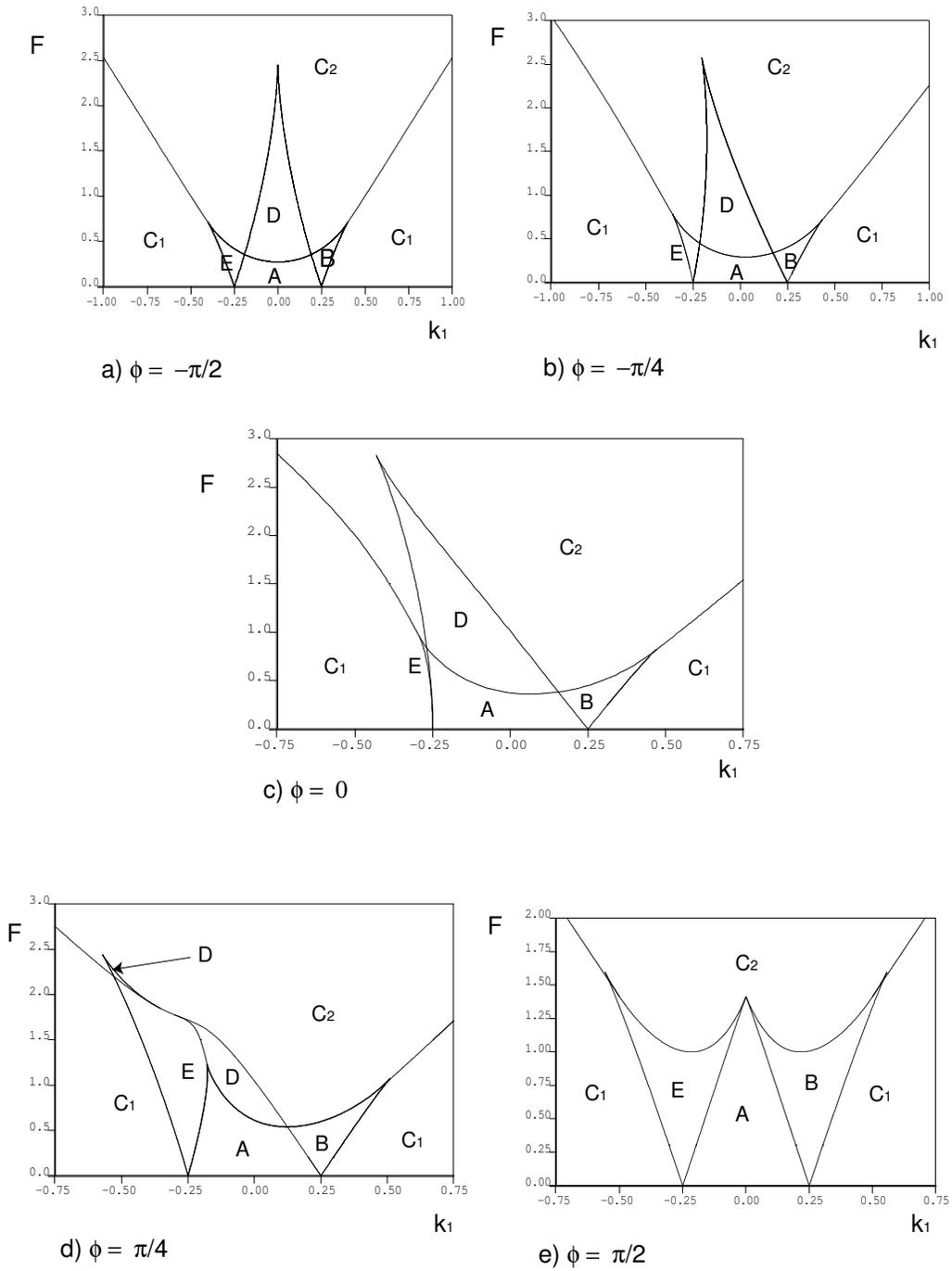
Figure 7. Bifurcation curves (obtained using AUTO) for slow flow 11,12 for $\phi = \frac{-\pi}{2}, \frac{-\pi}{4}, 0, \frac{\pi}{4}$ and $\frac{\pi}{2}$. $\alpha = 1$ in all the cases.